ORGANIC LETTERS

2006
Vol. 8, No. 17
3623−3626

Synthesis and Characterization of Glucosamine-Bound Near-Infrared Probes for Optical Imaging

Cong Li, Tiffany R. Greenwood, Zaver M. Bhujwalla, and Kristine Glunde*

JHU ICMIC Program, The Russell H. Morgan Department of Radiology and Radiological Science, Johns Hopkins University School of Medicine, Baltimore, Maryland 21205

kglunde@mri.jhu.edu

Received March 31, 2006

ABSTRACT

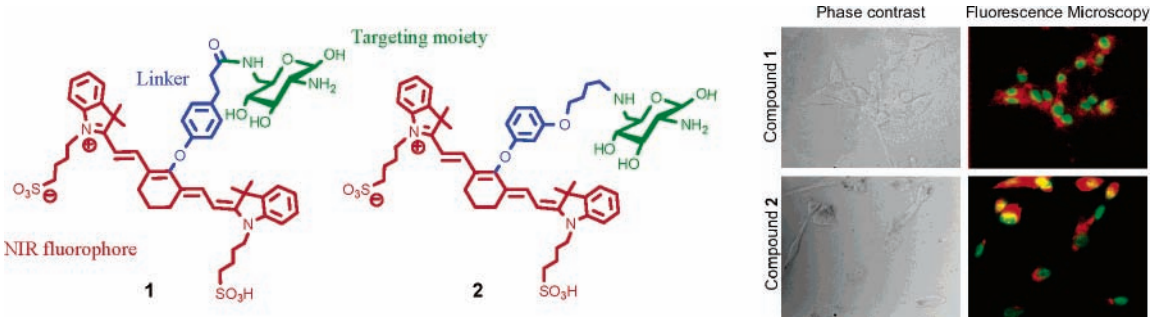

Two novel near-infrared (NIR) fluorescent probes have been synthesized by linking a carbocyanine fluorophore and glucosamine through different linkers. These probes demonstrated a high quantum yield, low cytotoxicity, reversible pH-dependent fluorescence in the physiological pH range, and a decreased aggregation tendency in aqueous solutions. In vitro NIR optical imaging studies revealed cellular uptake and strong intracellular NIR fluorescence of these two probes in four breast epithelial cell lines.

Optical imaging is an emerging noninvasive diagnostic imaging modality, which can be used for visualizing pathological conditions with high sensitivity, low tissue irradiation, and relatively low cost.[1] To this end, it is important to develop novel optical imaging probes and, in particular, probes that fluoresce in the near-infrared (NIR) wavelength range because tissue autofluorescence and light absorption in the NIR range (700−900 nm) are low, and NIR light can penetrate several centimeters into heterogeneous tissues.[2]

Lysosomes are membranous organelles found in almost all mammalian cells. Recent studies demonstrated that lysosomes can play a pivotal role in cancer cell invasion and metastasis because several crucial proteolytic enzymes, such as cathepsin D, B, and L, which actively participate in the digestion of extracellular matrix (ECM) proteins, are sequestered in lysosomal vesicles.[3] Moreover, under the conditions of acidic extracellular pH, which are frequently found in the tumor microenvironment, cells with a high degree of malignancy exhibited larger lysosome sizes and increased nucleus−lysosome distances than poorly metastatic cells.[4] Therefore, assessing lysosomal morphology and trafficking in vivo by using NIR optical imaging probes will help elucidate the role of lysosomal parameters in cancer invasion and metastasis and may provide a novel means of diagnosing malignant lesions in their early stages.[4,5]

(1) Shah, N.; Cerussi, A.; Eker, C.; Espinoza, J.; Butler, J.; Fishkin, J.; Hornung, R.; Tromberg, B. *Proc. Natl. Acad. Sci. U.S.A.* **2001**, *98*, 4420−4425.
(2) Achilefu, S. *Technol. Cancer Res. Treat.* **2004**, *3*, 393−409.
(3) (a) Roshy, S.; Sloane, B. F.; Moin, K. *Cancer Metastasis Rev.* **2003**, *22*, 271−86. (b) Levicar, N.; Strojnik, T.; Kos, J.; Dewey, R. A.; Pilkington, G. J.; Lah, T. T. *J. Neurooncol.* **2002**, *58*, 21−32.
(4) Glunde, K.; Guggino, S. E.; Solaiyappan, M.; Pathak, A. P.; Ichikawa, Y.; Bhujwalla, Z. M. *Neoplasia* **2003**, *5*, 533−545.
(5) Fehrenbacher, N.; Jaattela, M. *Cancer Res.* **2005**, *65*, 2993−2995.

10.1021/ol060783e CCC: $33.50
Published on Web 07/26/2006

We previously demonstrated that lysosomes can be optically imaged by covalently binding fluorophores to the C6 position of glucosamine.[6] Glucosamine is required for the biosynthesis of highly glycosylated lysosomal proteins, some of which are an integral part of lysosomal membranes.[7] Here, we report two novel compounds, in which a NIR fluorophore was covalently linked to glucosamine. Carbocyanine IR-783 (Figure 1) was chosen as a NIR fluorophore because of its

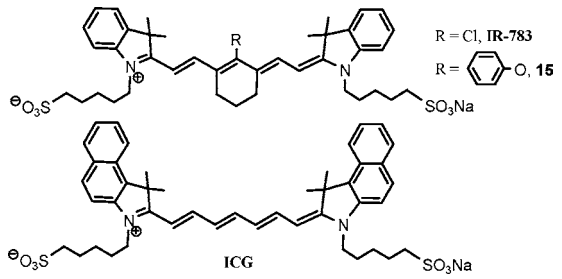

Figure 1. Chemical structures of IR-783, control molecule **15**, and indocyanine green (ICG).

high extinction coefficient, optimal emission wavelength, and good photochemical and photophysical stability.[8] To prevent self-quenching between carbocyanines in the cellular environment[9] and loss of bioactivity of the glucosamine due to modification with this bulky fluorophore,[10] two extended carbon chain linkers were placed between IR-783 and glucosamine.

The synthesis of compound **1** is outlined in Scheme 1. Bis-Boc-protected glucosamine **3** was prepared as previously described.[6] Regiospecific reaction of **3** with TsCl in pyridine achieved a monotosylation product at the C6 position. Replacement of tosyl with azide was achieved by treatment of **4** with sodium azide in DMF. Reduction of azide to amine was realized in THF/H_2O in the presence of triphenylphosphine. Treatment of 3-(4-hydrophenyl) propionic acid with *N*-hydrosuccinimide in the presence of DCC resulted in NHS-ester **7**,[11] which reacted efficiently with **6** to give **8**. Etherification of **8** with IR-783 was accomplished in DMF/NaH.[12] Deprotection of **9** was achieved in TFA/CH_2Cl_2, and the final product **1** was obtained as a deep green powder. Compound **2** was synthesized from **6** in five steps. The starting material 3-(4-iodobutoxy)-phenyl acetate **10** was prepared by reacting resorcinol monoacetate with 1,4-diiodobutane in acetone. Of

Scheme 1. Synthetic Procedures for Compounds **1** and **2**

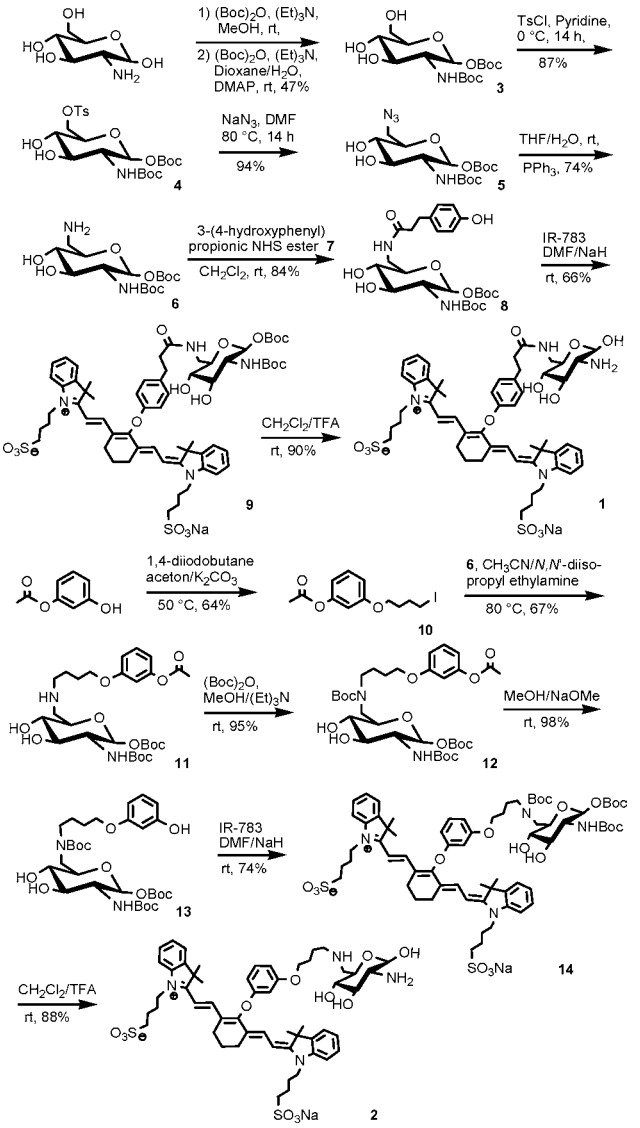

several possible reaction conditions to achieve alkylation between **10** and **6**, such as CH_3CN/K_2CO_3, $CH_3CN/(Et)_3N$, DMF/K_2CO_3, or CH_3CN/*N*,*N*′-diisopropyl ethylamine, only CH_3CN/*N*,*N*′-diisopropyl ethylamine provided the desired alkylated product **11** in modest yield. Treatment of **11** with $(Boc)_2O$ produced the fully protected tertiary amine **12**. Selective deprotection of the phenyl acetate in **12** was tested under different hydrolytic reaction conditions. In dioxane/NaOH or EtOH/NaOH, both the phenyl acetate and the *O*-Boc group at position C1 were hydrolyzed. The monohydrolytic product **13** was obtained in CH_3OH by applying a catalytic dose of CH_3ONa, giving a yield above 98%. Similar to **9**, **14** was prepared by treating **13** with IR-783.[12] Deprotection of **14** yielded **2** as a deep green solid. Additionally, to clearly identify the function of the glucosamine moiety in **1** and **2**, a control molecule **15**[13] (Figure 1), which has a fluorophore structure identical to that of **1** and **2**, was also prepared.

Photospectroscopic measurements performed in PBS at pH 7.4 revealed that the absorbances of **1** and **2** centered at 766

(6) (a) Glunde, K.; Guggino, S. E.; Ichikawa, Y.; Bhujwalla, Z. M. *Mol. Imaging* **2003**, *2*, 24−36. (b) Glunde, K.; Foss, C. A.; Takagi, T.; Wildes, F.; Bhujwalla, Z. M. *Bioconjugate Chem.* **2005**, *16*, 843−851.

(7) Winchester, B. *Glycobiology* **2005**, *15*, 1R−15R.

(8) (a) Hilderbrand, S. A.; Kelly, K. A.; Weissleder, R.; Tung, C.-H. *Bioconjugate Chem.* **2005**, *16*, 1275−1281. (b) Sasaki, E.; Kojima, H.; Nishimatsu, H.; Urano, Y.; Kikuchi, K.; Hirata, Y.; Nagano, T. *J. Am. Chem. Soc.* **2005**, *127*, 3684−3685.

(9) Weissleder, R.; Tung, C. H.; Mahmood, U.; Bogdanov, A., Jr. *Nat. Biotechnol.* **1999**, *17*, 375−378.

(10) Zhou, X. T.; Forestier, C.; Goff, R. D.; Li, C.; Teyton, L.; Bendelac, A.; Savage, P. B. *Org. Lett.* **2002**, *4*, 1267−1270.

(11) Suijkerbuijk, B. M. J. M.; Slagt, M. Q.; Klein Gebbink, R. J. M.; Lutz, M.; Spek, A. L.; van Koten, G. *Tetrahedron Lett.* **2002**, *43*, 6565−6568.

(12) Narayana, N.; Patonay, G. *J. Org. Chem.* **1995**, *60*, 2391−2395.

and 768 nm, with the corresponding emission maxima at 782 and 784 nm, respectively. Even though the molar extinction coefficients of **1** (ϵ = 176 000 M^{-1} cm^{-1}) and **2** (ϵ = 157 000 M^{-1} cm^{-1}) decreased compared to control molecule **15** (ϵ = 192 000 M^{-1} cm^{-1}) due to the "dye dilution" effect,[14] both of these new compounds demonstrated much higher quantum yields than **15** (0.043, Table 1). The

Table 1. Photophysical Properties of **1**, **2**, and **15**

	$\lambda_{max,abs}$ (nm)	ϵ (M^{-1} cm^{-1})	$\lambda_{max,\,em}$[a] (nm)[b]	Φ_f[b]
1[c]	766	176 000	782	0.186
2[c]	768	157 000	784	0.113
15[c]	766	192 000	783	0.043
ICG[c]	779	191 000	802	0.041
ICG[d]	794	218 000	816	0.13

[a] The fluorophores were excited at their maximum absorbances. [b] Quantum yields were determined by comparison with indocyanine green (ICG, Figure 1) in DMSO (Q.Y. = 0.13), at 298 K. [c] Measured in PBS buffer, pH 7.4 (<0.005% methanol as cosolvent). [d] Measured in DMSO.

fluorescence quantum yields (Φ_f) of **1** and **2** were 0.186 and 0.113, respectively, which correspond to a 4- and 3-fold increase compared to the control molecule. These high quantum yields of **1** and **2** can be explained by the presence of multiple hydrophilic groups in the glucosamine moiety, which may not only improve the hydrophilicity of these conjugates but also disrupt the $\pi-\pi$ interaction between the hydrophobic carbocyanine cores.[15] Reduced quantum yields of carbocyanine dyes in aqueous environments have previously been reported as a consequence of their self-aggregation.[15,16] To test this hypothesis, we studied the concentration dependence of the absorbances of **1**, **2**, and **15**. An additional broad, blue-shifted band centered at 670 nm increased with concentrations of **15** (Supporting Information, Figure S2), which most likely corresponded to H aggregates.[14] In contrast, no additional bands were found in the absorption spectra of **1** and **2**, not even at concentrations above 50 μM. These results indicate that **1** and **2** have decreased aggregation tendencies in aqueous solution compared to that of control molecule **15**.

To date, very few pH-dependent NIR dyes have been reported.[8b,17] pH effects on the fluorescence of **1** and **2** were investigated. Similar to control molecule **15**, the emission intensity of **1** decreased with acidification (Figure 2). Interestingly, compound **2** exhibited a quite unique pH-dependent fluorescence behavior. Between pH 11.0 and 7.2 (slope *a*, Figure 2), its fluorescence decreased significantly with decreasing pH, reaching a minimum at pH 7.2. Upon further acidification, the fluorescence increased inversely (slope *b*, Figure 2), reaching a maximum at pH 3.0 with a

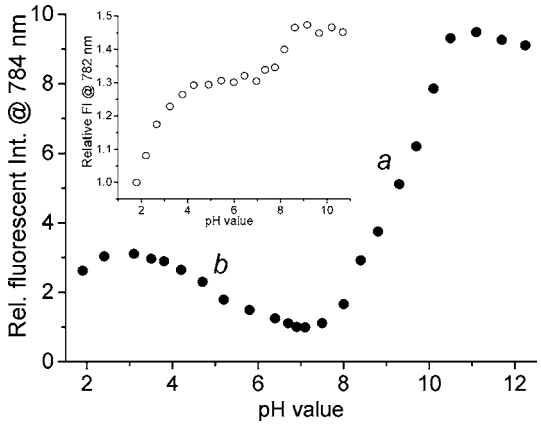

Figure 2. pH-dependent fluorescence intensity profile of **2** and **1** (inset) in 0.1 M sodium phosphate buffer. The fluorescence intensities of **2** and **1** (0.6 μM) were determined at 784 and 782 nm with excitation at 768 and 766 nm, respectively.

3-fold intensity enhancement compared to pH 7.2. This pH-dependent fluorescence was reversible in the pH range 3.0−7.0 for at least three cycles. Compound **2** may prove useful in future applications, where acidic environments, such as the lysosomal lumen (pH $\approx$ 5.0)[3,4] and/or the tumor microenvironment characterized by extracellular pH values of 6.4−6.8,[18] can enhance its NIR fluorescence. Intermolecular electrostatic repulsions arising from protonation of both secondary and primary amines in glucosamine may alleviate self-quenching between cyanine fluorophores and hence increase the fluorescence.

Previous studies reported that covalently binding saccharides to initially toxic polymers or small molecules can substantially decrease the toxicity of the resulting conjugates.[19] Here, we tested the cytotoxicity of **1** and **2** relative to **15** in four human mammary epithelial cell (HMEC) lines, MCF-12A, MCF-7, MDA-MB-231, and MDA-MB-435, which represent different stages of malignancy, by MTT assay.[20] In all four HMEC lines, **1** and **2** exhibited significantly lower cytotoxicity than **15**. No cells survived following treatment with **15** at concentrations above 250 μM. Compound **1** demonstrated minimal cytotoxicity, resulting in cell viabilities of 95%−100% in MCF-12A and MCF-7 cells even at the highest concentration (2.0 mM) (Figure 3). Although **1** and **2** exhibited minimal toxicity in MCF-7 and MCF-12A cells within the tested concentration range, both compounds caused significant cytotoxicity in the highly

(13) Gabor, P.; Narasimhachari, N.; Lucjan, S.; Lyle, R. M.; Malgorzata, L. US Patent 5,571,388, November 5, 1996.
(14) Ye, Y. P.; Li, W. P.; Anderson, C. J.; Kao, J.; Nikiforovich, G. V.; Achilefu, S. *J. Am. Chem. Soc.* **2003**, *125*, 7766−7767.
(15) (a) Khairutdinov, R. F.; Serpone, N. *J. Phys. Chem. B* **1997**, *101*, 2602−2610. (b) Egorov, V. V. *J. Chem. Phys.* **2002**, *116*, 3090−3103.
(16) Zhang, Z. R.; Achilefu, S. *Org. Lett.* **2004**, *6*, 2067−2070.
(17) Zhang, Z. R.; Achilefu, S. *Chem. Commun.* **2005**, 5887−5889.
(18) Stubbs, M.; McSheehy, P. M.; Griffiths, C. L. *Mol. Med. Today* **2000**, *6*, 15−19.
(19) (a) Metzke, M.; O'Connor, N.; Maiti, S.; Nelson, E.; Guan, Z. *Angew. Chem., Int. Ed.* **2005**, *44*, 6529−6533. (b) Queiroz, E. F.; Roblot, F.; Duret, P.; Figadère, B.; Gouyette, A.; Laprévote, O.; Serani, L.; Hocquemiller, R. *J. Med. Chem.* **2000**, *43*, 1604−1610.
(20) The MTT cell proliferation assay determines the ability of viable cells to reduce yellow [3-(4,5-dimethylthiazol-2-yl)-2,5-diphenyltetrazolium bromide] (MTT) to blue-colored formazan crystals by mitochondrial enzymes. The concentration of formazan crystals can be determined spectrophotometrically when dissolved in an organic solvent. For a detailed description of this assay, see: Cetin, Y.; Bullerman, L. B. *J. Agric. Food Chem.* **2005**, *53*, 6558−6563.

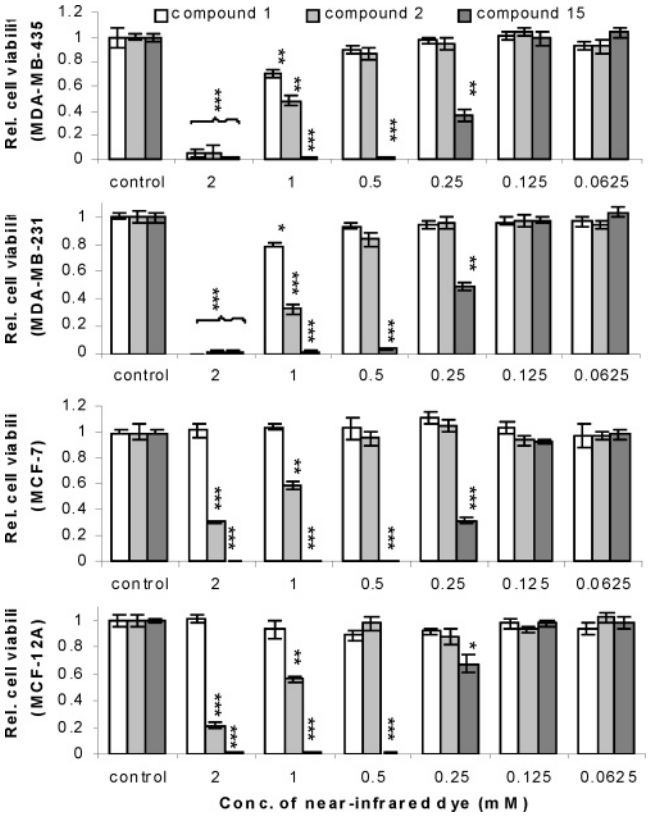

Figure 3. Relative cell viability of human MDA-MB-435 (n = 4), MDA-MB-231 (n = 8), MCF-7 (n = 8), and MCF-12A (n = 8) breast epithelial cells following 24 h of treatment with compounds **1** (white bars), **2** (light gray bars), and **15** (gray bars). Error bars represent mean ± SD, * indicates $P < 0.05$, ** indicates $P < 0.01$, and *** indicates $P < 0.001$ for relative cell viability after treatment with NIR dyes vs the control.

malignant cell lines MDA-MB-231 and MDA-MB-435 (cell viabilities ≤ 5%) when administered at a high concentration (2.0 mM). In contrast, **15** exhibited nonspecific cytotoxic behavior in all four HMEC lines. The low cytotoxicity of **1** and **2** may be due to multiple hydrophilic groups in glucosamine, which can shield surface charges of carbocyanine and thereby decrease potentially harmful Coulombic interactions of such dyes with cell membranes.[19a] Compounds **1** and **2** show great promise for future in vivo imaging applications because fluorescent probes are typically administered in a dose range between 0.1 and 600 μM.[6b,21]

NIR fluorescence microscopy demonstrated that **1** and **2** were taken up into the cells and resulted in strong intracellular NIR fluorescence in all four HMEC lines, as shown for MDA-MB-231 cells in Figure 4. Phase contrast images of the same fields of view revealed intracellular localization

(21) (a) Achilefu, S.; Bloch, S.; Markiewicz, M. A.; Zhong, T.; Ye, Y.; Dorshow, R. B.; Chance, B.; Liang, K. *Proc. Natl. Acad. Sci. U.S.A.* **2005**, *102*, 7976−7981. (b) Ye, Y.; Bloch, S.; Kao, J.; Achilefu, S. *Bioconjugate Chem.* **2005**, *16*, 51−61.

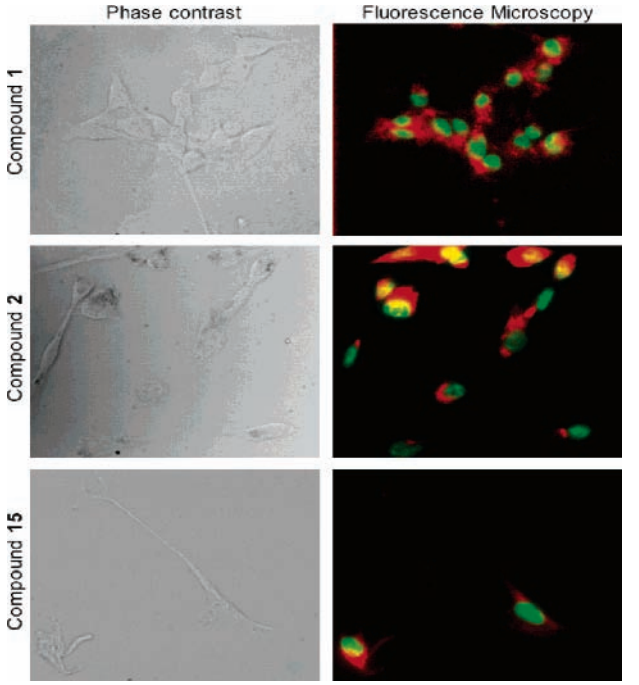

Figure 4. Phase contrast (left) and fluorescence (right) microscopy (40× lens) images of human MDA-MB-231 breast cancer cells following 24 h of treatment with 250 μM of **1** (top panel), **2** (middle panel), and control molecule **15** (bottom panel). NIR fluorescence is shown in red, and nuclei counterstain with Hoechst-33342 is displayed in green.

of **1** and **2**. NIR fluorescence (red) of **1** was localized in small intracellular vesicles, and a partially punctate pattern was detected for **2**, most likely attributable to lysosomal localization. NIR fluorescence from control molecule **15** was detected predominantly in dead cells and weakly in live cells without giving a punctate pattern.

In summary, we have developed two novel NIR fluorescent probes, which demonstrated high quantum yields, low cytotoxicity, reversible pH-dependent fluorescence, and a low tendency to aggregate in aqueous solution. Incubation of HMEC cultures with **1** or **2** resulted in cellular uptake of these compounds and intense punctate intracellular NIR fluorescence. In vivo NIR optical imaging studies with **1** and **2** are currently underway.

Acknowledgment. This work was supported by R21 CA112216 and P50 CA103175. We thank Dr. Paul Winnard and Dr. Noriko Mori for technical assistance.

Supporting Information Available: Experimental procedures, full characterization of compounds **1**, **2**, and **15**, photospectroscopic analysis, pH-dependent fluorescence, in vitro cytotoxicity studies, and fluorescence microscopy. This material is available free of charge via the Internet at http://pubs.acs.org.

OL060783E